Geophysical measurements for site response investigation: preliminary results on the island of Malta

F. Panzera[1], S. D'Amico[2], P. Galea[2], G. Lombardo[1], M.R. Gallipoli[1,3] and S. Pace[2]

[1] Dipartimento di Scienze Biologiche, Geologiche e Ambientali, Università di Catania, Italy
[2] Department of Physics, University of Malta, Msida, Malta
[3] Istituto di Metodologia per le Analisi Ambientali, CNR, Tito Scalo, Italy

ABSTRACT   The main goal of this study is to investigate the dynamic properties of main lithotypes outcropping on the island of Malta and to evaluate the general features of the local seismic response through the combined use of geophysical methods based on Rayleigh waves and horizontal to vertical noise spectral ratios. These kind of studies have unfortunately never been undertaken in Malta and, therefore, no shear wave velocity values and fundamental frequency of outcropping lithotypes have been published. The proposed preliminary results represent a valid set of data useful for evaluating seismic hazard and risk for the Maltese islands. Even if the seismic activity around the archipelago is generally of low to moderate magnitude the islands in the past were struck by large events in Sicily and the Hellenic arc resulting in considerable damage.

1. Introduction

Geophysical approaches to seismic hazard estimation usually have an important role in the estimate of the risk in terms of the probability that a given magnitude earthquake may occur in a given area within a fixed period of time. Another important issue is the mapping of site amplification effects as recently asserted by Parolai et al. (2007). In recent times, rather than using a simple descriptor, such as "rock" or "non-rock", as usually introduced in the ground motion prediction equation to take into account site effects, more refined indicators of site geology features have been adopted. It is indeed possible to quantify the modification of the ground motion according to the site geology, by using, for instance, a distinction between thin and thick deposits, or evaluating the S-wave velocity. A widely applied parameter is the mean value of shear wave velocity over the first 30 m ($V_{S,30}$), which is used to classify soils into a small number of classes in both the Italian and European seismic codes (Eurocode8, 2003; Ministero dei Lavori Pubblici, 2008). Although statistical tests would conclude that this parameter has a weak link to seismic amplification (Castellaro et al., 2008; Gallipoli and Mucciarelli, 2009) it is, however, commonly used for quick characterization of the seismic properties of lithotypes.

Non-invasive geophysical prospecting techniques, based on surface wave dispersion properties in vertically heterogeneous media, are also largely adopted to estimate $V_{S,30}$ through an inversion processes (Herrmann, 1994; Wathelet et al., 2005). The Multichannel Analysis of Surface Waves (MASW) technique proposed by Park et al. (1999) is amongst the most widely used methods. Another important tool for the seismic characterization of shallow geological

structures is provided by the Horizontal to Vertical Noise spectral Ratio (HVNR) technique. This technique, firstly introduced by Nogoshi and Igarashi (1971), was put into practice by Nakamura (1989) and became in recent years widely used since it provides a good estimate of the fundamental frequency of soft soil deposits (e.g., Al Yuncha *et al.*, 2004; Vuan *et al.*, 2008; Albarello *et al.*, 2011). The basic hypothesis for using ambient noise is that the resonance of a soft layer corresponds to the fundamental mode of Rayleigh waves, which is associated with an inversion of the direction of Rayleigh waves rotation (Nogoshi and Igarashi, 1971; Lachet and Bard, 1994). It is commonly accepted that, although the single components of ambient noise can show large spectral variations as a function of natural and cultural disturbances, the HVNR spectral ratio tends to remain invariant, therefore preserving the fundamental frequency peak (Cara *et al.*, 2003). Although many authors (e.g., Mucciarelli, 1998; Rodriguez and Midorikawa, 2002; Maresca *et al.*, 2003) have questioned the existence of simple direct correlation between HVNR amplitude values and the site amplification, this method is widely used for the significantly reduced field data acquisition time and costs. Unfortunately these studies have never been undertaken in Malta so that no $V_{S,30}$ values and fundamental frequencies of outcropping lithotypes were up to now investigated. The Maltese islands are exposed to a low-to-moderate seismic hazard. The data reported in Galea (2007) testify that a number of felt events can be attributed to major earthquakes located either in Sicily (e.g., 1693 VII-VIII MCS intensity) or in southern Greece (e.g., 1856 VI-VII MCS intensity), but many others are linked to offshore earthquakes having epicentres in the Sicily Channel (e.g., 1923 VI MCS intensity). All these events affected the country in past centuries and caused considerable damage.

A culture of seismic risk awareness has never really been developed in the country, and the public perception is that the islands are relatively safe, and that any earthquake phenomena are mild and infrequent. This is probably due to the fact that no large loss of life has ever been documented as a direct result of earthquake activity, and the last occurrence of serious damage to buildings was almost a century ago (Galea, 2007). The general public perception is thus one of unjustified complacency, and no comprehensive assessment of seismic risk has so far been carried out even though much of the building stock is of load-bearing unreinforced masonry, and is vulnerable to even moderate ground shaking.

The present study will address the component of seismic risk arising from local site amplification, which is the result of the particular local sedimentary geology. It aims at investigating the dynamic properties of main lithotypes outcropping on the island of Malta and to evaluate the general features of the local seismic response through the combined use of methods based on Rayleigh waves and HVNR Non-invasive seismic prospecting techniques (MASW), using the vertical component of surface waves, were applied in 8 sites, selected among the mostly outcropping lithotypes, to estimate the dispersion curves and the shear-wave velocity profiles in the upper 30 m. Moreover, ambient noise measurements were performed to infer shallow shear wave velocity structure as well as a preliminary evaluation of the site response in 16 sites, processing the data through spectral ratio techniques (HVNR).

2. Geological setting

Malta is located in the southern Mediterranean area and it is mostly composed of marine

sedimentary rocks (Fig. 1a). The oldest sedimentary formation of the Maltese Islands, of Triassic age, is not outcropping and the main exposed rocks were deposited from the Oligocene-Miocene to Quaternary periods. The litho-stratigraphic sequence (Fig. 1b) is relatively simple, consisting of five major layers namely the Lower Coralline Limestone (LCL), the Globigerina Limestone (GL), the Blue Clay (BC), the Greensand Formation and the Upper Coralline Limestone (UCL). UCL, GL and LCL strata are essentially considered as being stiff rocks, whereas the BC and the Greensands are soft sediments (Pedley *et al.*, 1978, 2002).

The LCL is the oldest exposed rock in the Maltese Islands, outcropping to a height of 140 m in the vertical cliffs near Xlendi (Gozo). GL is the second oldest rock and outcrops over approximately 70% of the area of the islands. On weathering and erosion, it assumes a broad gently rolling landscape. The thickness of this formation changes considerably, ranging from 23 m near Fort Chambray (Gozo) to 207 m around Marsaxlokk (Malta). The BC formation overlies the GL. It erodes easily when wet and it forms taluses which flow out over the underlying rock. Variations in thickness are considerable, ranging from 75 m at Xaghra (Gozo) to nil in eastern Malta. Greensand consists of bioclastic limestones rich in glauconite that were deposited in a warm sea. Unweathered sections are green but they are oxidised to an orange color when exposed. The deposit attains a maximum thickness of 11 m in localised depressions at Il-Gelmus in Gozo, but elsewhere is less than 1 m thick. UCL is the youngest Tertiary formation in the islands, reaching a thickness of approximately 160 m in the Bingemma area (Malta). Local tectonic activity appears to have resulted in the brief emergence of the formation above the sea. The strata are very similar to the lowest stratum in the Maltese Islands. These rocks are sporadically overlain by terrestrial, Aeolian and alluvial deposits laid down following the emergence of the Maltese Islands above sea level (hereafter indicated as Soil and Detritus formation, SD). Much of the central and south-eastern portion of Malta comprises outcrops of GL while the northern and north-western regions are characterized by highlands on which UCL is the dominant outcrop. The geology of Gozo is more varied than that of Malta, with more frequent outcrops of BC being a characteristic feature.

3. Methodology

3.1. MASW technique

The dynamic properties of the main lithotypes outcropping in the study area were evaluated through the non-invasive technique MASW. This technique needs a suitable location of the seismic source as well as a correct choice of transducers spacing in order to define a reliable wave-length range in the measurements. The dispersion curves are always obtained in a relatively high frequency range (5–50 Hz), that implies a maximum depth of investigation usually not exceeding 30 m, depending on the lithotype features and the active sources used. It is also of crucial importance to adopt the ideal distance for the nearest offset (source-to-nearest receiver distance) and for the maximum offset (source-to-farthest receiver distance) for a correct investigation depth (Park *et al.,* 2002). A longer receiver spread is, indeed, necessary for the lower frequencies component of surface waves, but if the maximum receiver offset is too large (> 100 m), the high-frequency components of surface-wave energy will be poorly defined in the spectrum (Park *et al.,* 1999).
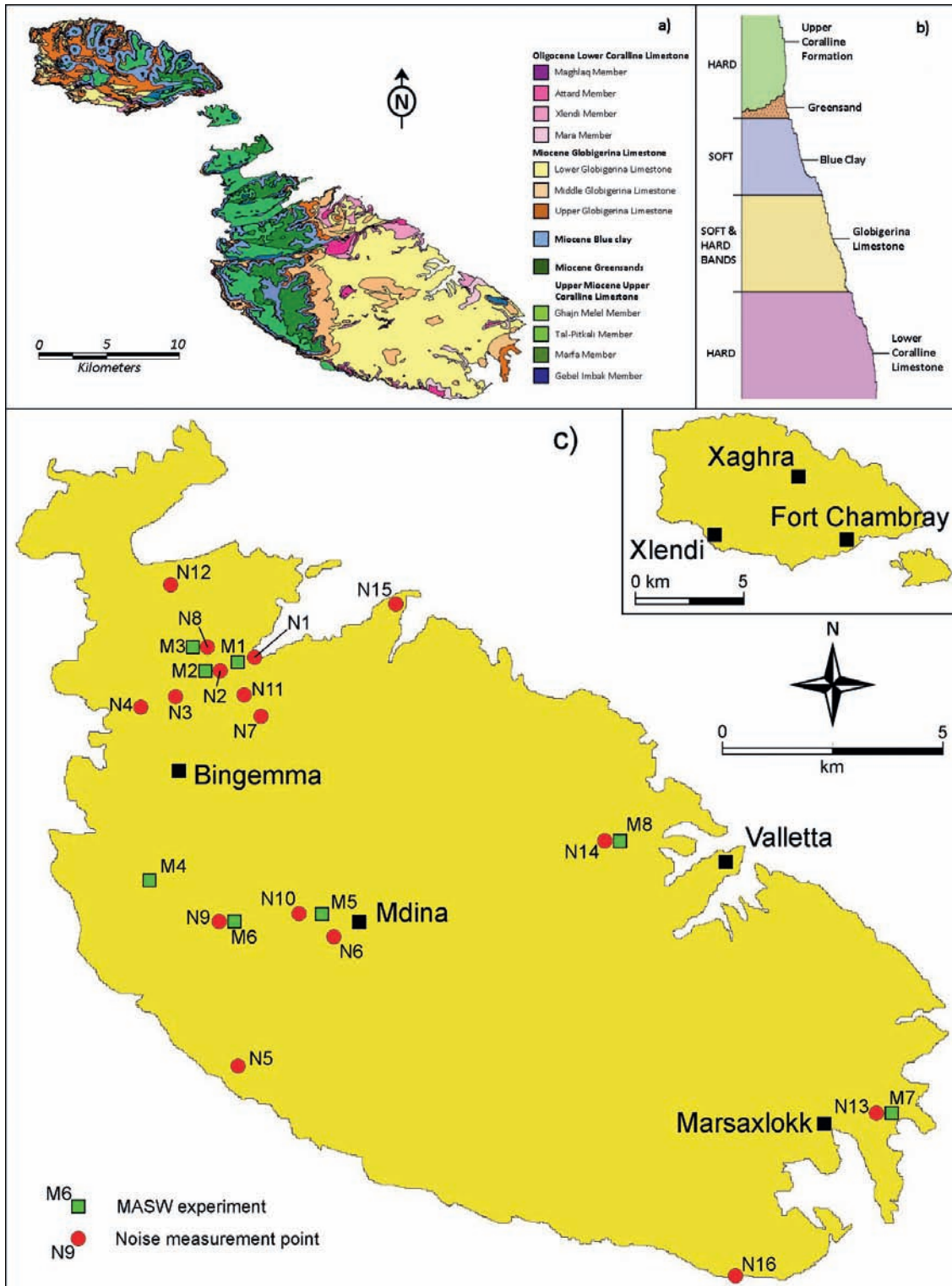
Fig. 1 – a) Geo-lithologic map of the island of Malta (modified from Pedley *et al.*, 1978, 2002); b) schematic stratigraphic geological sequence in the Maltese Islands; c) location of the measurement sites (see Table 1 for further details).

Table 1 - Location of MASW and HVNR measurement points.

MASW investigated sites				
id	Latitude	Longitude	Site name	Lithotype
M1	35.944924°	14.380087°	Xemxija	SD
M2	35.942404°	14.373625°	Xemxija	SD
M3	35.946610°	14.371050°	Xemxija	UCL
M4	35.893088°	14.359260°	Kuncizzjoni	UCL
M5	35.886527°	14.401677°	Mdina	BC
M6	35.886514°	14.376997°	Rabat	BC
M7	35.843587°	14.562408°	Marsaxlokk	GL
M8	35.901313°	14.484159°	Msida	GL
HVNR investigated sites				
id	Latitude	Longitude	Site name	Lithotype
N1	35.945140°	14.382839°	Xemxija	SD
N2	35.942800°	14.377846°	Xemxija	SD
N3	35.935872°	14.359149°	Golden Bay	SD
N4	35.934802°	14.353217°	Golden Bay	SD
N5	35.854019°	14.380125°	Dingli	UCL
N6	35.886460°	14.402960°	Mdina	UCL
N7	35.932710°	14.386400°	Wardija	UCL
N8	35.946610°	14.371050°	Xemxija	UCL
N9	35.886514°	14.376997°	Rabat	BC
N10	35.886527°	14.401677°	Mdina	BC
N11	35.937430°	14.381758°	Wardija	BC
N12	35.962210°	14.361505°	Melliha	BC
N13	35.843587°	14.562408°	Marsaxlokk	GL
N14	35.901313°	14.484159°	Msida	GL
N15	35.957310°	14.422400°	Qwara	GL
N16	35.806766°	14.517759°	Bizerbbuga	LCL

MASW tests, in present study, were performed using a 12-channel seismograph equipped with 4.5 Hz geophones. A linear array having a length of 48 m, depending on the available free space at each site, was deployed using a 4 m interval pitch between the sensors. An 8 kg hammer source, with a fixed 10 m offset distance was used, recording five shots, 3 s length, with a sample rate of 512 Hz.

MASW experimental dispersion curves were carried out using the Grilla 6.1 software (www.tromino.eu). The software calculates the *f-k* spectrum of a seismic section, having the travel time (*t*) and the distance (*x*) as the vertical and the horizontal coordinates, respectively. The transform of *t* gives the frequency spectrum and the transform of the *x* coordinate gives the wavenumber *k* spectrum (Lacoss *et al.*, 1969; Kvaerna and Ringdahl, 1986). From the *f-k* spectrum the phase velocity vs. frequency contour plot (Fig. 2), was obtained for the eight

investigated sites (Fig. 1c and Table 1). The obtained dispersion curves were automatically picked from the displayed trends, sampling a large number of apparent phase velocities. The automatic picking of the dispersion curve of each site was approximated through a regression to a polynomial curve of fourth/sixth degree according to the observed trend (Fig. 3) following a method similar to the one proposed by Coccia *et al.* (2010).

In surface-wave inversion, we have tried to use higher modes because, in several real cases, the experimental dispersion curve is the result of the superposition of several modes, particularly when velocity inversions or strong velocity contrasts are present in the S-wave profile (Maraschini *et al.*, 2010). Higher modes are sensitive to parameters to which the fundamental mode is poorly sensitive (Socco and Strobbia, 2004) and their inclusion in the inversion process will improve the accuracy of the result (Ernst, 2008; Maraschini *et al.*, 2010). Including higher modes can also increase the investigation depth (Gabriels *et al.*, 1987) when the low-frequency band is not available (Ernst, 2008), can stabilize the inversion process (Xu *et al.*, 2006), and can enhance the resolution of the inverted model. The derivation of one-dimensional shear-wave velocity profiles from surface wave dispersion curves is a classical inversion problem in geophysics. The inversion of dispersion curves is known to be strongly nonlinear and is affected by non-uniqueness of solutions (Dal Moro *et al.*, 2006). In the present study, the Rayleigh wave dispersion curves, obtained from the experimental setup, were inverted using the DINVER software (www.geopsy.org) which provided a set of dispersion curve models compatible with the observed dispersion one. This inversion tool uses a directed-search method, called *"neighbourhood algorithm"* (Sambridge, 1999; Wathelet *et al.*, 2005; Wathelet, 2008), for nonlinear inversion that employs the Voronoi cells to investigate the multidimensional model and to compute the misfit function across the parameter space. The misfit function between experimental and computed dispersion curves is defined for each inverted model as:

$$misfit_{disp} = \sqrt{\sum_{i=0}^{n_f} \frac{\left(x_{exp} - x_{cal}\right)^2}{\sigma_i^2 n_f}} \tag{1}$$

where x_{exp} and x_{cal} are the phase velocities of the experimental and the calculated curves at frequency f_i, σ_i is the uncertainty of the considered frequency samples and n_f is the number of frequency samples. As suggested by Wathelet (2008), since in the present study the uncertainty was not considered, σ_i was replaced by x_{exp}.

An approximate knowledge of the free parameters is necessary in order to invert the experimental dispersion curve. This can be obtained using information coming either from a preliminary geological survey or from borehole data. If not, this information can be directly deduced from the fundamental mode of the Rayleigh wave dispersion curves. Following the suggestions of several authors (Konno and Kataoka, 2000; Martin and Diehl, 2004; Albarello and Gargani, 2010), the average S-wave velocity, up to a depth *h*, almost corresponds to the Rayleigh waves phase velocity relative to a fixed wavelength of the order of 1-3 times *h*. To invert the dispersion curve, a set of 2-5 uniform layers with homogeneous properties was considered, taking into account five parameters: shear wave velocity (V_S), thickness (H), compressional wave velocity (V_P), Poisson's ratio (v) and density (ρ). The most influent parameter in the surface wave inversion process is V_S, which, for all layers, was allowed to range between 100-2000 m/s. The
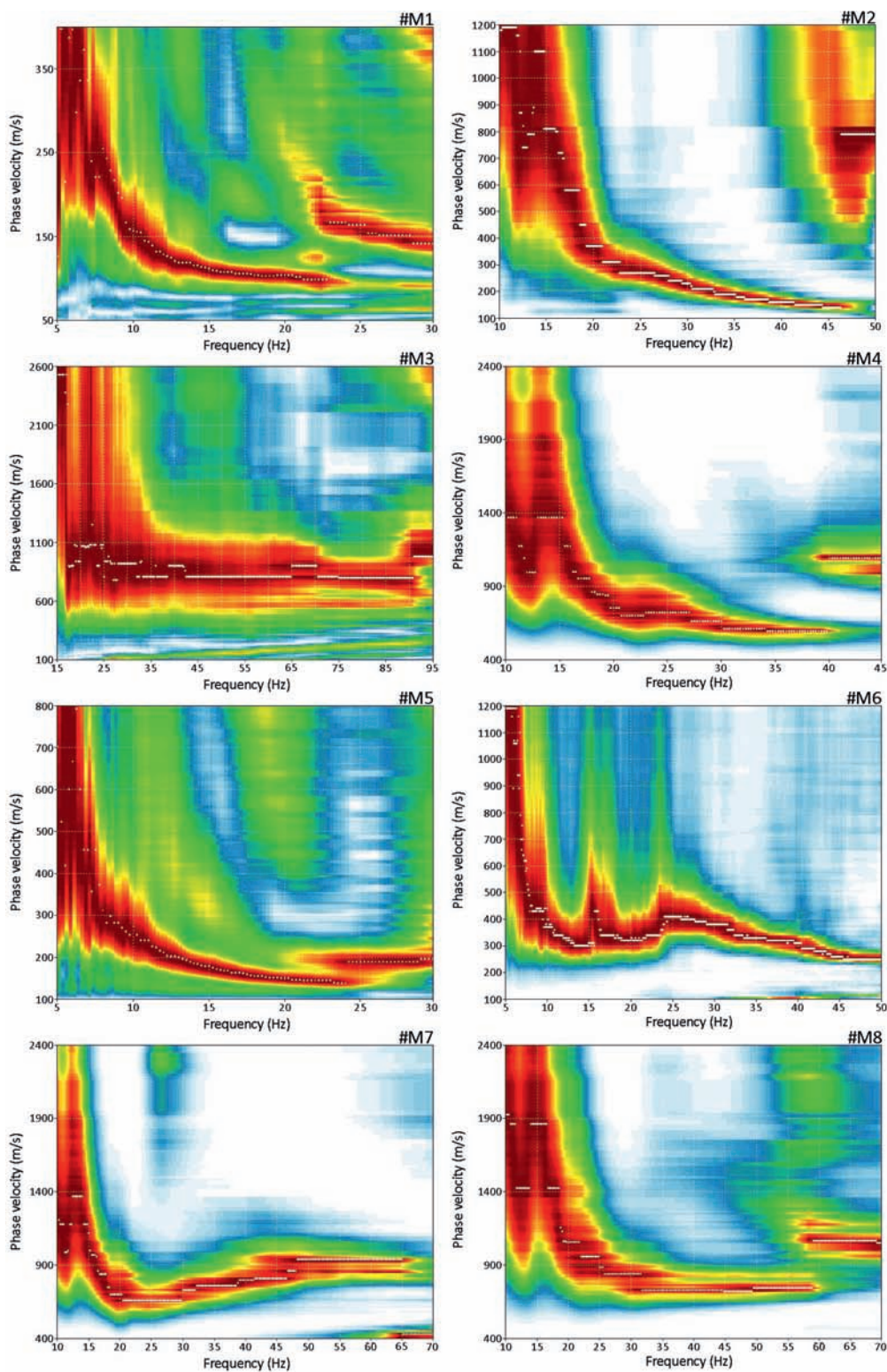
Fig. 2 - Phase velocity vs. frequency contour plot spectra for MASW experiments performed in the eight considered measurement sites.
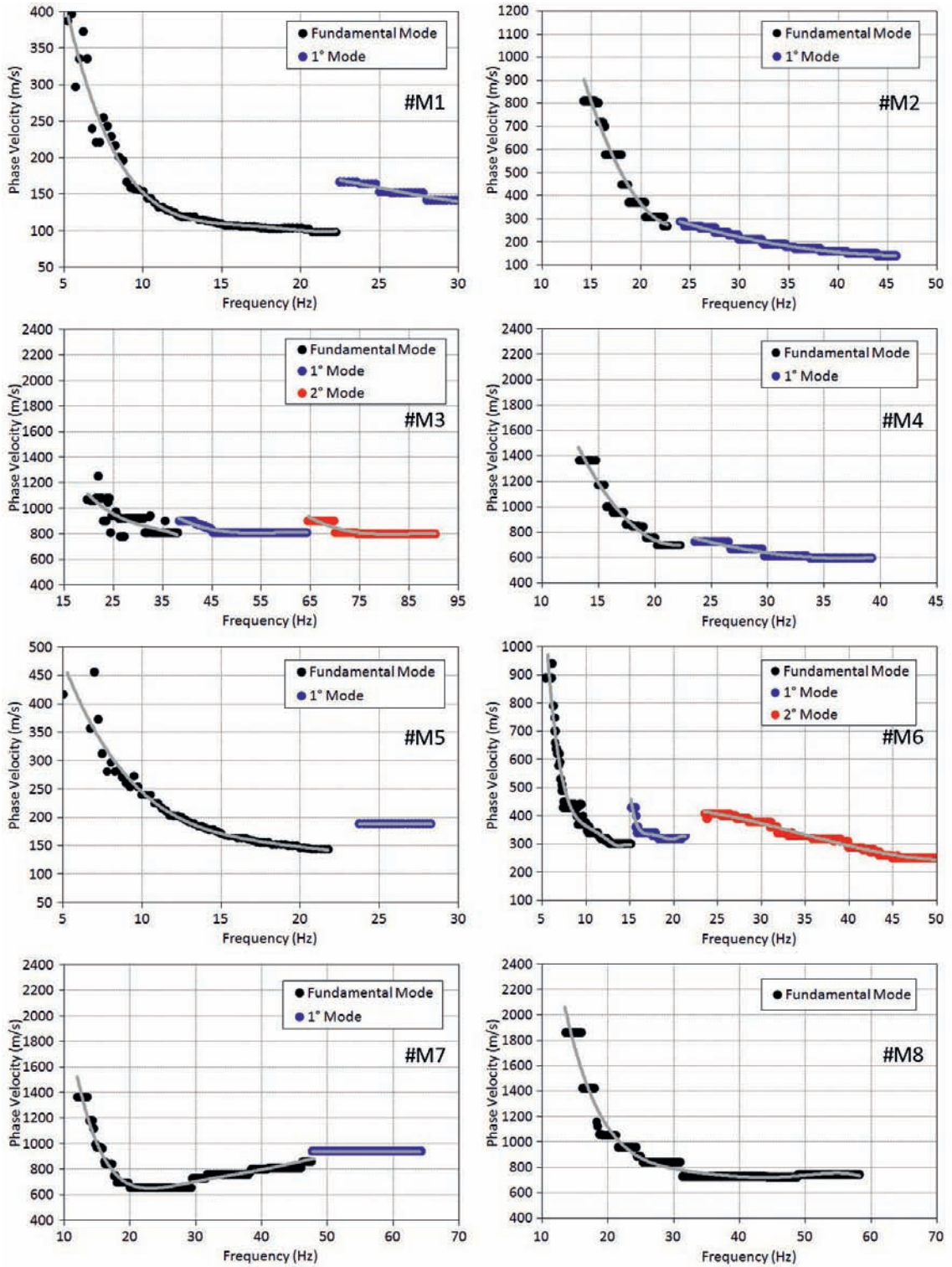
Fig. 3 - Polynomial regression curves obtained from the automatic picking of Fig. 2 plots.

Table 2 - Input parameters used for the inversion of the experimental dispersion curves at each investigated site.

			MASW			
SITE	N° Layer	V_P (m/s)	σ	V_S (m/s)	H (m)	ρ(kg/m³)
M1	1	160-370	0.2-0.4	100-150	1-5	1900
	2	240-500	0.2-0.4	150-200	5-8	1900
	3	320-860	0.2-0.4	200-350	12-15	1900
	4	970-2200	0.2-0.4	600-900	∞	1900
M2	1	80-370	0.2-0.4	50-150	0-2	1900
	2	320-740	0.2-0.4	200-300	4-6	1900
	3	1400-2700	0.2-0.4	900-1100	?	1900
M3	1	800-1700	0.2-0.4	500-700	1-5	1900
	2	1300-2200	0.2-0.4	800-900	10-15	1900
	3	1790-2400	0.2-0.4	1100-1200	15-20	1900
	4	1950-3400	0.2-0.4	1200-1400	∞	1900
M4	1	480-860	0.2-0.4	300-350	1-5	1900
	2	980-1950	0.2-0.4	600-800	15-20	1900
	3	2400-3900	0.2-0.4	1400-1600	∞	1900
M5	1	160-500	0.2-0.4	100-200	1-4	1900
	2	240-860	0.2-0.4	150-350	4-8	1900
	3	480-1200	0.2-0.4	300-500	12-15	1900
	4	800-1700	0.2-0.4	500-700	∞	1900
M6	1	160-370	0.2-0.4	100-150	1-5	1900
	2	240-610	0.2-0.4	150-250	5-10	1900
	3	480-980	0.2-0.4	300-400	14-18	1900
	4	970-1950	0.2-0.4	600-800	∞	1900
M7	1	890-1600	0.2-0.4	550-650	1-4	1900
	2	2100-3700	0.2-0.4	1300-1500	5-8	1900
	3	650-1200	0.2-0.4	400-500	12-15	1900
	4	1100-2200	0.2-0.4	700-900	15-20	1900
	5	2400-4000	0.2-0.4	1500-1700	∞	1900
M8	1	1100-2200	0.2-0.4	700-900	10-20	1900
	2	2400-4400	0.2-0.4	1400-1800	∞	1900

influence of the other parameters is relatively small (Xia *et al.*, 1999, 2003; Wathelet, 2008). For this reason, consistently with its low influence on surface wave dispersion, the density (ρ) was fixed at a constant value of 1900 kg/m³ in each layer. The compressional velocity (V_P) was varied from 100 to 4000 m/s and the Poisson's ratio (v) was ranging between 0.2 and 0.4. As regards the thickness (*H*) it was constrained by fixing the bottom depths of some layers. Generally, the thickness limits are defined through the wavelengths (λ) derived from the frequencies and phase-velocities of the experimental dispersion curves. The thickness range was obtained considering $\lambda/4$ and $\lambda/2$ for the minimum and maximum bottom depth, respectively. Table 2 shows the inversion parameters used for each layer.

3.2. HVNR technique

The HVNR method is a common tool, used for site effect investigations, based on the ratio of horizontal over vertical spectral components of motion. Generally, this spectral ratio exhibits a peak, that corresponds more or less to the fundamental frequency of the site

(Bonnefoy-Claudet *et al.*, 2006). However, the ambient noise wavefield is the result of the combination of unknown portions of both body and surface waves. If the first are prevailing, the ratio is mainly induced by S_H resonance in the superficial layers whereas, if Rayleigh surface waves predominate, the theoretical ellipticity dictates the observed curves (Nogoshi and Igarashi, 1971; Fäh *et al.*, 2001; Scherbaum *et al., 2003*). This is especially true when a large shear-wave velocity contrast exists between the shallow layer and the bedrock, as theoretically confirmed by Malischewsky and Scherbaum (2004). Although experimental data peaks usually fit quite well the frequency of the theoretical curves, they are far less reliable as regards their amplitude. Nevertheless, the HVNR contains valuable information about the underlying structure, especially as regards the relationship between V_S of the sediments and their thickness (Ibs-Vonseth and Wholenberg, 1999; Scherbaum *et al., 2003*).

The ambient noise was recorded in 16 sites (Fig. 1c and Table 1) using Tromino (www.tromino.eu), a compact 3-component velocimeter. Time series of ambient noise, having a length of 20 minutes, were recorded with a sampling rate of 128 Hz. Following the guidelines suggested by the SESAME (2004) project the recorded signal was divided in non-overlapping time windows of 20 s. For each window a 5% cosine taper was applied and the Fourier spectra were calculated. The spectra of each window were smoothed using a Konno-Ohmachi window (Konno and Ohmachi, 1998) fixing the parameter *b* to 40. Finally the resulting HVNR, in the frequency range 0.5-20.0 Hz, was computed estimating the logarithmic average of the spectral ratio obtained for each time window, selecting only the most stationary and excluding transients associated to very close sources.

Moreover, HVNRs were also obtained in the MASW selected sites using them to estimate the ellipticity curves aiming at improving the final solution of the dispersion curves inversion. It is indeed well known that the HVNR information usually control the deeper part of the estimated V_s profiles. The ellipticity estimate was performed taking into account only the fitting with the dominant peak frequency because the absolute amplitude of the curve could be affected by the features of the noise wavefield. The ellipticity-based method provides good results only when sources are near and in those sites presenting a strong S-wave velocity contrast between sediments and bedrock (Bonnefoy-Claudet *et al.*, 2006). At such sites, the HVNR shows a strong peak. The misfit function between the frequency of the peak of HVNR and the computed ellipticity is defined as:

$$misfit_{ellip} = \frac{f_{exp} - f_{cal}}{df_{exp}} \qquad\qquad (2)$$

where f_{exp} is the frequency of the peak, and df_{exp} is the standard deviation of the experimental frequency peak. In case a joint inversion of the dispersion curve and the frequency peak of the ellipticity is performed, the two misfits are combined using the following relation:

$$misfit_{global} = (1-\alpha)\ misfit_{disp} + \alpha\, misfit_{ellip}. \qquad\qquad (3)$$

4. Results and discussion

The use of techniques based on the propagation of surface waves made possible to detect the

$V_{S,30}$ features of the main outcropping lithotypes and consequently the classification, according to the Eurocode8 (2003), of the investigated sites.

In Fig. 4a, the results of the dispersion curve inversion process, performed through the *"neighborhood algorithm"*, are shown for sites #M1 and #M2, both located on the SD formation. This lithotype, which is the product of the erosion of carbonate present on the island of Malta, can reach thicknesses of about 10-15 m and outcrops especially in the grabens of the northern part of the island. These sediments are not reported in the official geological map but we preferred in any case to characterize their features for the seismic site response evaluation, performing two MASW experiments. A good fit between experimental and theoretical dispersion curves was obtained and $V_{S,30}$ values of 308 m/s and 557 m/s, were obtained from the MASW prospections. Such results allow us to classify these sites as belonging to the C and B soil categories, respectively. The ellipticity of the theoretical fundamental mode of Rayleigh waves (Fig. 4a), obtained considering the best inverted model from MASW, is consistent in terms of fundamental frequency with the HVNR peak. This indicate that the #M1 and #M2 sites are characterized by a simple 1D layering with a strong velocity contrast between the soft sediments outcropping (SD) and the underlying formation (UCL).

The features of UCL formation, which is considered as being stiff rock, were investigated performing MASW experiments in the sites #M3 and #M4 (see Fig. 1c). The dispersion curves are well defined for frequency higher than 10 Hz, with velocities approximately ranging between 550 and 1400 m/s and higher vibration modes are also identifiable (Fig. 4b). The results of the dispersion curve inversion show $V_{S,30}$ values of about 1047 m/s and 765 m/s, respectively, classifying both the considered sites in the A soil category. As previously stated, outcrops of the SD formation are often observed to overly the UCL especially in the northern part of the island. The presence of such lithotype produces a drastic reduction of the $V_{S,30}$ values (see Fig. 4a). For this reason it would be important to investigate the effects of the SD presence and to evaluate if its thickness has a significant influence in evaluating the site response, especially in the urban areas. The experimental HVNR curves are not fully matched from the theoretical ellipticity, especially at low frequencies, mainly because there is lack of phase velocity estimates at low frequency values (Fig. 4b).

A good match between experimental and theoretical dispersion curves is observed for the MASW performed in the sites #M5 and #M6 located on the BC formation (Fig. 5a) and the obtained inversion model provides $V_{S,30}$ values of 390 m/s and 327 m/s, respectively. The results of the dispersion curves inversion suggest a C soil category for these sites. The results of ellipticity (Fig. 5a) do not totally fit the HVNR fundamental peak observed in the MASW experimental sites. This could be explained as a consequence of a bedrock depth greater than the one obtained through the experimental dispersion curve. Underneath a depth of 15-25 m, the inverted velocity profile is indeed not well constrained, considering the used experimental setup. However, the MASW experiments highlight the presence of a discontinuity within the BC. A longer linear array spacing and the use of lower frequency geophones could have improved the resolution at greater depth (>15-25 m).

Finally, the results of MASW measurements performed on the GL formation are depicted in Fig. 5b (#M7, #M8). The rather good misfit value (0.01-0.05) obtained from the inversion process allowed us to obtain $V_{S,30}$ values ranging between 902 m/s and 1020 m/s. Such values are typical
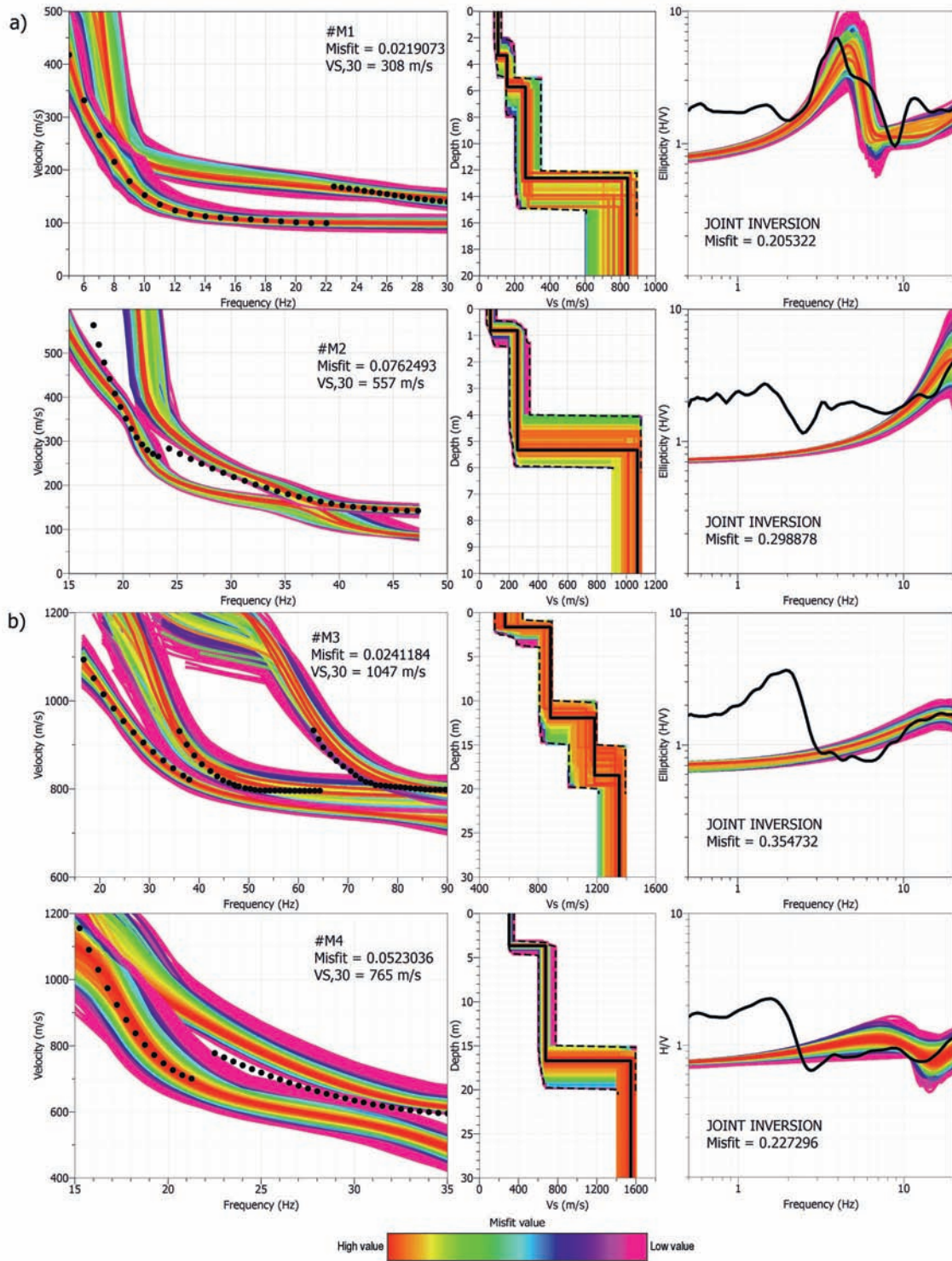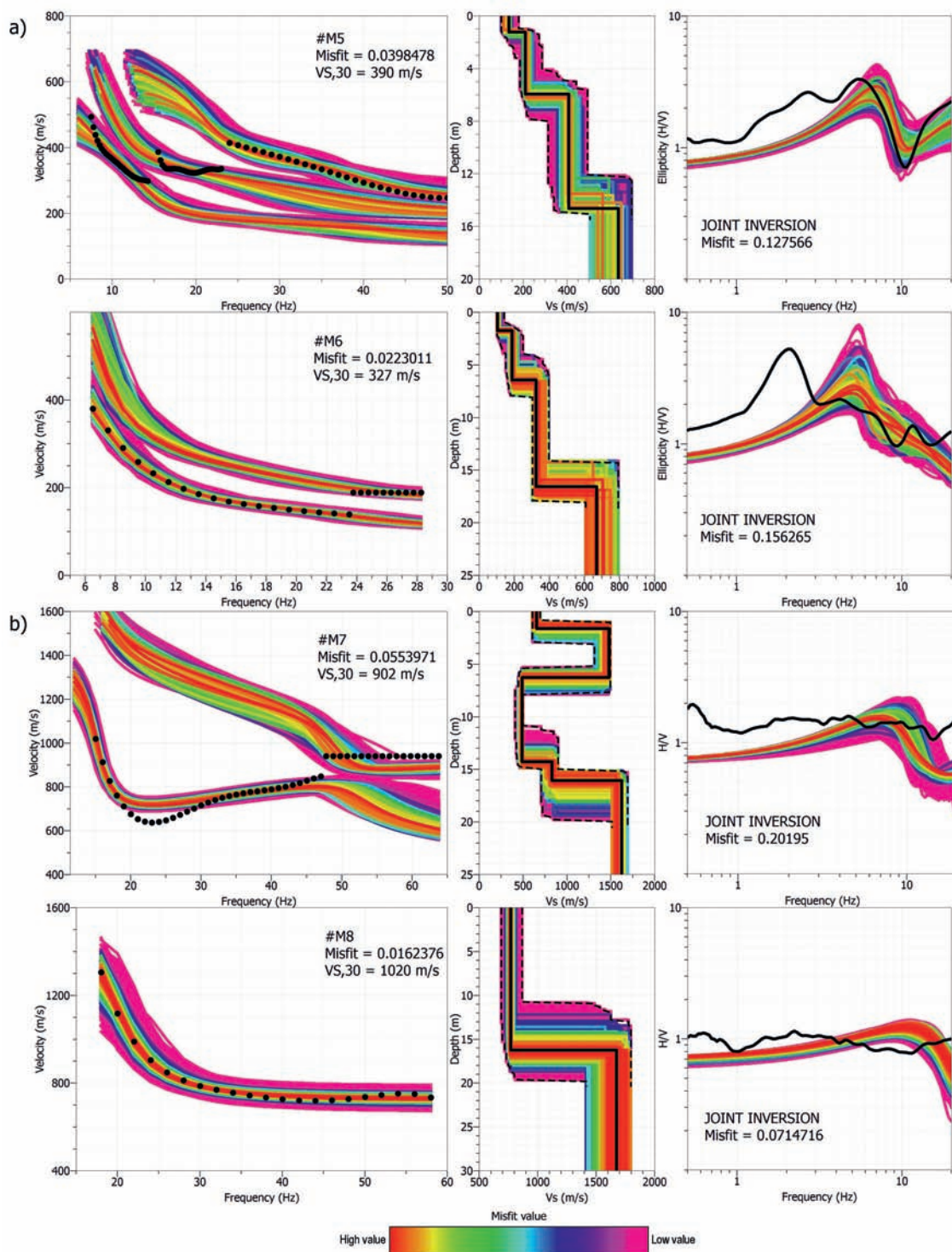
Fig. 4 - Dispersion curves, shear wave velocity profiles and ellipticity curves obtained from the joint inversion of the experimental phase velocities (black dots) and the HVNR curves (black lines) from measurement sites located on the SD formation (a) and the UCL formation (b); black lines in the V_s profiles indicates the best estimated model.

Fig. 5 - Dispersion curves, shear wave velocity profiles and ellipticity curves obtained from the joint inversion of the experimental phase velocities (black dots) and the HVNR curves (black lines) from measurement sites located on the BC formation (a) and the GL (b); black lines in the V_s profiles indicates the best estimated model.

of A class category. The GL formation may indeed be considered as the bedrock for the Maltese Islands. It is worth to comment on the results for #M7, which show quite a distinct velocity inversion. This may be explained by the fact that in this particular site, the outcropping lithotype is the Upper GL Member, which is underlain by the Middle GL Member, a softer carbonate mudstone, often described as "marly". Since the Upper GL layer is only around 5 m thick, the effect is evident in the dispersion curves and the resulting velocity model. The experimental HVNR curves are not fully matched from the theoretical ellipticity. This, in our opinion, could be a consequence of the lack of an appropriate velocity contrast within the investigated lithotype (GL).

The fundamental frequencies of 16 sites, selected according to easy access criteria on the main lithotypes cropping out on Malta, were evaluated through a series of ambient noise measurements. Fig. 6 shows the set of results for all the different outcrops. SD formation shows pronounced spectral ratio peaks that appear shifting in frequency according to the thickness of such soft sediments overlying the limestone. Though the observed fundamental frequencies often are at relatively high values (#N2, #N3) the thickness of such formation appears not negligible (> 10 m) and extremely variable, especially along the coast, where it gives rise to dominant peaks at frequency lower than 4.0 Hz (#N1, #N4). The UCL sites are characterized by spectral ratio peaks in the frequency range 1.0-3.0 Hz (see Fig. 6b) that could be related to the presence of a BC layer between the UCL and GL formations as demonstrated by Panzera *et al.* (2012). There are practical implications for such findings since it appears evident that a more simplified amplification study like $V_{S,30}$ would fail to predict the observed site-response behaviour in the presence of a velocity inversion. For UCL formation, a $V_{S,30}$ about 900 m/s is indeed obtained and an A soil category is assigned although, as here observed, HVNR point out the existence of significant peaks that could be ascribed to possible amplification phenomena. As concerns the BC formation, the results set into evidence the presence of pronounced spectral peaks similarly to what has been observed in the recording sites located on the SD sediments. The BC formation has an average thickness of about 40-50 m and consequently its fundamental frequency ranges at values between 1.0 and 8.0 Hz that are, of course, not negligible from the engineering point of view. Finally, the measurements performed on the GL depict a flat shape of the spectral ratios, which support the statement that the GL formation can be considered as the local bedrock. It has to be specified that the #N16 site is located on the LCL that represent the deeper stratigraphic level cropping out in some spots only.

It is worth noting that HVNR depicted in Fig. 6 summarize, from lower to higher panels, the stratigraphic sequence typical of Malta Island. It appears clear that, apart from GL formation, all the other lithotypes show significant spectral ratio peaks having amplitude higher than two units. This observation could represent a useful clue in order to preliminarily characterize the local seismic response as a function of the outcropping lithotypes. If we have a look at the geologic map, we notice that in the north-western portion of Malta Island, where younger formations outcrop, site effects are more evident than in the south-eastern part of the island, where the GL is widely outcropping. Similar findings were described by Galea (2007), analyzing the macroseismic intensity data and should be further supported by increasing the ambient noise measurement sites in order to be able to set into evidence the variability of the fundamental frequency and realize an iso-frequency contour map.
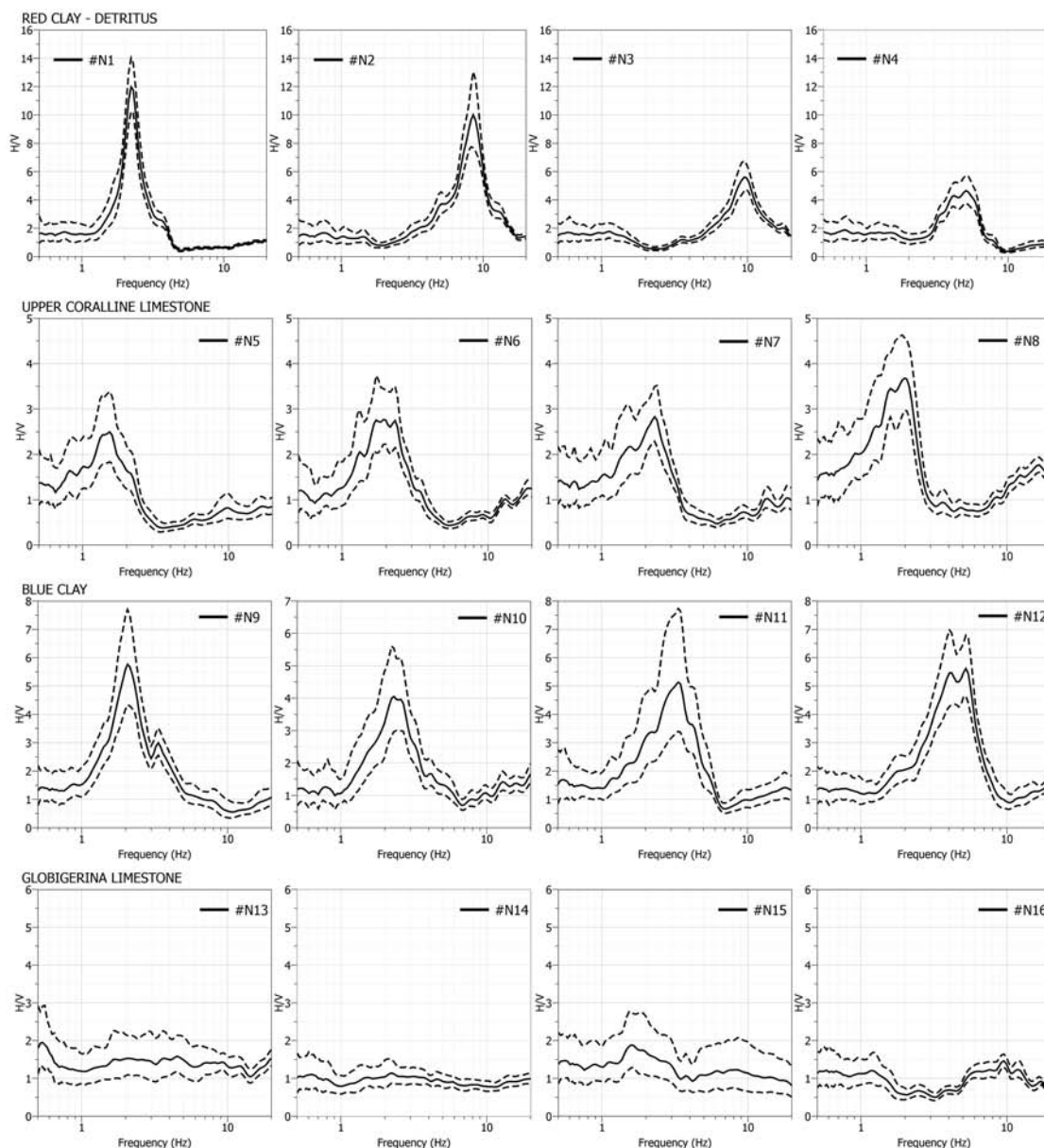
Fig. 6 - HVNR from measurements performed on the main lithotypes outcropping on Malta Island; dotted lines refer to standard deviation.

5. Concluding remark

A preliminary study to evaluate the problems related to investigation of the local seismic response in the island of Malta was performed using a twofold approach based on the multichannel analysis of Rayleigh waves (MASW) and HVNR spectral ratios. Such approach

allowed also testing the reliability of the widely used $V_{S,30}$ estimate in order to classify the lithotypes outcropping in Malta Island, where no seismic code is up to now adopted.

The inversion of the dispersion curves obtained from surface wave propagation allowed us to obtain a good characterization of $V_{S,30}$ features for the main lithotypes. HVNR pointed out the frequency range values that can be associated to such lithotypes.

Findings from the two different approaches show a general good agreement. Low shear wave velocities in the BC and in the SD formations match up to more pronounced HVNR peaks whereas high $V_{S,30}$ values are observed for limestone, where no significant spectral ratio peaks appear evident. We can therefore assert that the GL can be considered as the local bedrock whereas major amplifications occur on soft soils.

A fitting between the HVNR frequency peaks and the theoretical ellipticity was however performed in order to get information about the deeper part of the estimated V_s profiles, testing at the same time if the depth reached through the investigations was adequate to characterize the considered lithotypes. The results showed that the linear array length and consequently the investigated depth were sometimes not adequate. Such observation taught us that it would be particularly important to perform the ambient noise survey prior to carrying out the MASW prospections. This can, indeed, give useful hints for a correct planning of the array length as well as the source receivers offset (Panzera and Lombardo, 2012). Particular attention should indeed be paid to the site response evaluation on the UCL formation. The HVNR curves show for such lithotype significant peaks in the frequency range 1.0-3.0 Hz whereas $V_{S,30}$ values (750-1100 m/s) are typical of a rock type formation. These spectral ratio features appear related to the presence of a BC layer interbedded between the UCL and GL formations. It is therefore advisable, in order to improve the quality of the parameters necessary for a characterization of the local seismic response, to increase the investigated depth, especially in the north-western part of the island.

In conclusion, a tendency towards a greater amplification of site effects was observed in the western part of the island where a top layer of UCL overlies the BC soft formation. In a recent paper, Galea (2007) set into evidence that major effects of historical earthquakes have affected this portion of the island (Mdina) as well as Gozo. In the frame of present results, we think that the observation of such greater damage is related rather than to the location of seismic sources, to the different geologic setting of the two parts of the island of Malta. The local geology seems therefore to play an important role.

REFERENCES

Albarello D. and Gargani F.; 2010: *Providing NEHRP soil classification from the direct interpretation of effective Rayleigh waves dispersion curves.* Bull. Seismol. Soc. Am., **100**, 3284–3294, doi:10.1785/0120100052.

Albarello D., Cesi C., Eulilli V., Guerrini F., Lunedei E., Paolucci E., Pileggi D. and Puzzilli L.M.; 2011: *The contribution of the ambient vibration prospecting in seismic microzoning: an example from the area damaged by the April 6, 2009 L'Aquila (Italy) earthquake.* Boll. Geof. Teor. Appl., **52**, 513-538.

Al Yuncha Z., Luzon F., Posadas A., Martin J., Alguacil G., Almendros J. and Sanchez S.; 2004: *The use of ambient seismic noise measurements for the estimation of surface soil effects: the Motril city case (Southern Spain).* Pure Appl.

Geophys., **161**, 1549–1559.

Bonnefoy-Claudet S., Cornou C., Bard P.Y., Cotton F., Moczo P., Kristek J. and Fäh D.; 2006: *H/V ratio: a tool for site effects evaluation. Results from 1-D noise simulations*. Geophys J. Int., **167**, 827–837, doi:10.1111/j.1365-246X.2006.03154.x

Cara F., Di Giulio G. and Rovelli A.; 2003: *A study on seismic noise variations at Colfiorito, Central Italy: implications for the use of H/V spectral ratios*. Geophysical Research Letters, **30**, 1972-1976.

Castellaro S., Mulargia F. and Rossi P.M.; 2008: *VS30: proxy for seismic amplification?* Seism. Res. Lett., **79**, 540–542.

Coccia S., Del Gaudio V., Venisti N. and Wasowski J.; 2010: *Application of Refraction Microtremor (ReMi) technique for determination of 1-D shear wave velocity in a landslide area*. J. Appl. Geophys., **71**, 71–89.

Dal Moro G., Pipan M. and Gabrielli P.; 2006: *Rayleigh wave dispersion curve inversion via genetic algorithms and marginal posterior probability density estimation*. Geophysics, **61**, 39–55, doi:10.1016/j.appgeo.2006.04.002.

Ernst F.; 2008: *Multi-mode inversion for P-wave velocity and thick near-surface layers*. In: Proc. Near Surface Conference, EAGE, Extended Abstracts, A13.

Eurocode8; 2003: *Design of structures for earthquake resistance—Part 1: general rules, seismic actions and rules for buildings*. EN 1998, European Committee for Standardization, Brussels.

Fäh D., Kind F. and Giardini D.; 2001: *A theoretical investigation of average H/V ratios*. Geophys. J. Int., **145**, 535–549.

Gabriels P., Snieder R. and Nolet G.; 1987: *In situ measurements of shear wave velocity in sediments with higher-mode Rayleigh waves*. Geophysical Prospecting, **35**, 187–196.

Galea P.; 2007: *The seismic history of the Maltese Islands and considerations on seismic risk*. Annals of Geophysics, **50**, 725-740.

Gallipoli M.R. and Mucciarelli M.; 2009: *Comparison of site classification from VS30, VS10, and HVSR in Italy*. Bull Seism Soc Am., **99**, 340-351.

Herrmann R.B.; 1994: *Computer programs in seismology*. Vol. IV, St. Louis University, St. Louis (Missouri), U.S.A.

Konno K. and Kataoka S.; 2000: *An estimating method for the average S-wave velocity of ground from the phase velocity of Rayleigh wave*. In: Proceedings of JSCE, 647, pp. 415–423.

Konno K. and Ohmachi T.; 1998: *Ground-motion characteristics estimated from spectral ratio between horizontal and vertical components of microtremor*. Bull. Seism. Soc. Am., **88**, 228–241.

Kvaerna T. and Ringdahl F.; 1986: *Stability of various fk-estimation techniques, in Semiannual Technical Summary, 1 October 1985 - 31 March 1986*. In: NORSAR Scientific Report, 1-86/87, Kjeller, Norway, pp. 29-40.

Ibs-Von Seth M. and Wohlenberg J.; 1999: *Microtremor measurements used to map thickness of soft sediments*. Bull. Seism. Soc. Am., **89**, 250–259.

Lachet C. and Bard P.Y.; 1994: *Numerical and theoretical investigations on the possibilities and limitation of the Nakamura technique*. J. Phys. Earth., **42**, 377–397.

Lacoss R.T., Kelly E.J. and Toksöz M.N.; 1969: *Estimation of seismic noise structure using arrays*. Geophysics, **34**, 21-38.

Malischewky P.G. and Scherbaum F.; 2004: *Love's formula and H/V ratio (ellipticity) of Rayleigh waves*. Wave Motion, **40**, 57–67.

Maraschini M., Ernst F., Foti S. and Socco L.V.; 2010: *A new misfit function for multimodal inversion of surface waves*. Geophysics, **75**, 31-43.

Maresca R., Castellano M., De Matteis R., Saccorotti G. and Vaccariello P.; 2003: *Local site effects in the town of Benevento (Italy) from noise measurements*. Pure Appl. Geophys., **160**, 1745–1764.

Martin A.J. and Diehl J.G.; 2004: *Practical experience using a simplified procedure to measure average shear wave velocity to a depth of 30 meters (VS30)*. In: 13th World Conference on Earthquake Engineering, Vancouver, B.C., Canada, August 1–6, 2004, paper n. 952.

Ministero dei Lavori Pubblici; 2008: *Norme tecniche per le costruzioni*. Gazzetta Ufficiale della Repubblica Italiana, 29.

Mucciarelli M.; 1998: *Reliability and applicability of Nakamura's technique using microtremors: an experimental approach*. J. Earth. Eng., **2**, 625–638.

Nakamura Y.; 1989: *A method for dynamic characteristics estimation of sub surface using microtremor on the surface*. Railw. Tech. Res. Inst. Rep., **30**, 25–33

Nogoshi M. and Igarashi T.; 1971: *On the amplitude characteristic of microtremor (part 2) (in Japanese with English abstract)*. J. Seism. Soc. Japan, **24**, 26–40.

Panzera F. and Lombardo G.; 2012: *Seismic property characterization of lithotypes cropping out in the Siracusa urban area, Italy.* Engineering Geology, doi: 10.1016/j.enggeo.2012.11.011.

Panzera F., D'Amico S., Lotteri A., Galea P. and Lombardo G.; 2012: *Seismic site response of unstable steep slope using noise measurements: the case study of Xemxija bay area, Malta.* Nat. Hazards Earth Syst. Sci., **12**, 3421–3431, doi:10.5194/nhess-12-3421-2012.

Park C.B., Miller R.D. and Miura H.; 2002: *Optimum field parameter of a MASW survey*. In: Proc. Society of Exploration Geophysicists of Japan, Tokio, May 22-23, Extended Abstract.

Park C.B., Miller R.D. and Xia J.; 1999: *Multichannel analysis of surface waves*. Geophysics, **64**, 800–808.

Parolai S., Grünthal G. and Wahlström R.; 2007: *Site-specific response spectra from the combination of microzonation with probabilistic seismic hazard assessment—an example for the Cologne (Germany) area*. Soil Dyn. Earthq. Eng., **27**, 49–59.

Pedley H.M., Clark M. and Galea P.; 2002: *Limestone isles in a cristal sea: the geology of the Maltese islands*. P.E.G. Ltd, ISBN: 99909-0-318-2.

Pedley H.M., House M.R. and Waugh B.; 1978: *The geology of the Pelagian block: the Maltese Islands*. In: Narin A.E.M., Kanes W.H. and Stehli F.G. (eds), The Ocean Basin and Margins. Vol. 4B: The Western Mediterranean, Plenum Press, London, pp. 417-433.

Rodriguez V.H. and Midorikawa S.; 2002: *Applicability of the H/V spectral ratio of microtremors in assessing site effects on seismic motion*. Earthquake Eng. Struct. Dyn., **31**, 261–279.

Sambridge M.; 1999: *Geophysical inversion with a neighbourhood algorithm: I. Searching a parameter space*. Geophys. J. Int., **138**, 479– 494.

Scherbaum F., Hinzen K.G. and Ohrnberger M.; 2003: *Determination of shallow shear wave velocity profiles in the Cologne, Germany area using ambient vibrations*. Geophys J. Int., **152**, 597–612.

SESAME; 2004: *Guidelines for the implementation of the H/V spectral ratio technique on ambient vibrations: measurements, processing and interpretation*. SESAME European Research Project WP12, deliverable D23.12, http://sesame-fp5.obs.ujf-grenoble.fr/Deliverables/Del-D23-HV_User_Guidelines.pdf.

Socco L.V. and C. Strobbia; 2004: *Surface wave methods for near-surface characterisation: A tutorial*. Near Surface Geophysics, **2**, 165–185.

Vuan A., Priolo E., Restivo A., Barnaba C., Laurenzano G., Michelini A., Di Bartolomeo P. and Romanelli M.; 2008: *Site response estimation in the Vittorio Veneto area (N.E. Italy) Part 1: geophysical measurements and in situ soil characterization*. Boll. Geof. Teor. Appl., **49**, 369-386

Wathelet M.; 2008: *An improved neighborhood algorithm: parameter conditions and dynamic scaling*. Geophys. Res. Lett., **35**, L09301, doi:10.1029/2008GL033256.

Wathelet M., Jongmans D. and Ohrnberger M.; 2005: *Direct inversion of spatial autocorrelation curves with the neighborhood algorithm*. Bull. Seism. Soc. Am., **95**, 1787-1800.

Xia J., Miller R.D. and Park C.B.; 1999: *Estimation of near-surface shear-wave velocity by inversion of Rayleigh wave*. Geophysics, **64**, 691-700.

Xia J., Miller R.D., Park C.B. and Tian G.; 2003: *Inversion of high frequency surface waves with fundamental and higher modes*. J. Appl. Geophys., **52**, 45–57.

Xu Y., Xia J. and Miller R.D.; 2006: *Quantitative estimation of minimum offset for multichannel surface-wave survey with actively exciting source*. Journal of Applied Geophysics, **59**, 117–125.

Corresponding author: Francesco Panzera
                          Università degli Studi di Catania, Dipartimento di Scienze Biologiche, Geologiche ed Ambientali
                          Sezione di Scienze della Terra
                          Corso Italia 57, 95129 Catania, Italy
                          Phone: +39 095 7195706; fax: +39 095 7195760; e-mail: panzerafrancesco@hotmail.it